


Please cite the Published Version

Abelmann, L, Porthun, S, Haast, M, Lodder, C, Moser, A, Best, ME, Van Schendel, PJA, Stiefel, B, Hug, HJ, Heydon, GP, Farley, A, Hoon, SR , Pfaffelhuber, T, Proksch, R and Babcock, K (1998) Comparing the resolution of magnetic force microscopes using the CAMST reference samples. Journal of Magnetism and Magnetic Materials, 190 (1-2). pp. 135-147. ISSN 0304-8853

DOI: [https://doi.org/10.1016/S0304-8853\(98\)00281-9](https://doi.org/10.1016/S0304-8853(98)00281-9)

Publisher: Elsevier

Version: Accepted Version

Downloaded from: <https://e-space.mmu.ac.uk/550057/>

Usage rights:  [Creative Commons: Attribution-Noncommercial-No Derivative Works 4.0](#)

Additional Information: This is an Accepted Manuscript of a work that was accepted for publication in Journal of Arid Environments. Changes resulting from the publishing process, such as editing, corrections, structural formatting, and other quality control mechanisms may not be reflected in this document. Changes may have been made to this work since it was submitted for publication.

Enquiries:

If you have questions about this document, contact openresearch@mmu.ac.uk. Please include the URL of the record in e-space. If you believe that your, or a third party's rights have been compromised through this document please see our Take Down policy (available from <https://www.mmu.ac.uk/library/using-the-library/policies-and-guidelines>)

Comparing the resolution of Magnetic Force Microscopes using the
CAMST Reference Samples

**Leon Abelmann¹, Steffen Porthun^{1*}, Marc Haast¹, Cock Lodder¹, Andreas
Moser², Margaret E. Best², Pieter J.A. van Schendel³, Bruno Stiefel³, Hans J.
Hug³, Greg P. Heydon^{4**}, Andrew Farley^{4***}, Steve R. Hoon⁴, Thomas
Pfaffelhuber⁶, Roger Proksch⁷, Ken Babcock⁷**

¹ *MESA Research Institute, University of Twente, Enschede, The Netherlands*

² *IBM Almaden Research Center, San Jose, USA*

³ *Institute of Physics, University of Basel, Basel, Switzerland*

⁴ *School of Physics, Manchester Metropolitan University, Manchester, UK*

⁶ *Department of Applied Physics, University of Regensburg, Regensburg, Germany*

⁷ *Digital Instruments, Santa Barbara, USA*

1. Abstract

A set of reference samples for comparing the results obtained with different Magnetic Force Microscopes (MFM) has been prepared. These samples consist of CoNi/Pt magneto-optic multilayers with different thickness. The magnetic properties of the multilayer are tailored in such a way that a very fine stripe domain structure occurs in remanence. On top of this intrinsic domain structure, bits were written thermomagnetically using different laser powers. These samples have been imaged in six different laboratories employing both home-built and commercial magnetic force microscopes. The resolution obtained with these different microscopes, tips and measurement methods varies between 30 and 100 nm.

Keywords: Magnetic Force Microscopy, resolution, fourier analysis, low temperature, vacuum, magneto-optic.

Contact author:

Leon Abelman
Information Storage Technology Group
MESA Research Institute, University of Twente
PoBox 217, 7500 AE Enschede, The Netherlands

Tel: xx-31-534892699 (office) or xx-31-534891043 (lab)
Fax: xx-31-534893343
E-Mail: L.Abelmann@el.utwente.nl

Changes of addresses:

(*Now at RHK, Rochester Hills, USA **Now at Sheffield University, Sheffield, UK

***Now at Oxford Instruments, Cambridge, UK)

2. Introduction

In the period between 1995 and 1997 the Conserted Action on Magnetic Storage Technology program (CAMST) of the European Community organised a number of small workshops and an internet conference on Magnetic Force Microscopy (MFM) instrumentation. In view of their scope, these meetings were mostly attended by researchers constructing their own MFMs. At the first meeting it was agreed that there was a need for a standard magnetic sample on which the instrumentation and scanning modes could be tested and compared to other instruments. As a result a series of standard samples, known as the CAMST reference samples, was prepared at the MESA institute of the University of Twente in the Netherlands.

Since then, commercial MFMs have developed to a high level of sensitivity and reliability. The operators of these instruments also felt the need to compare their instruments, and more important, their tips with other instruments and tips. In this paper the first results of the comparison of both home-made and commercial MFMs are presented. By no means is this paper meant as an overview, a large number of samples are still under investigation in laboratories not mentioned in this paper and it is foreseen that more results will follow. In this paper we will focus on the comparison of maximum obtainable resolution of the different systems

3. Sample description

Some criteria and demands which can be formulated for reference sample are

- there should be many copies which should be as identical as possible
- they should be relatively easy to prepare in large quantities

- the sample should contain structures varying in size and periodicity from large to very small
- the sample should be a well understood and physically and chemically stable

These demands are fulfilled by a thin film multilayer system which was developed for magneto-optic recording at shorter laser wavelengths (Blue laser diodes) [1]. These multilayers, which consist of $\text{Co}_x\text{Ni}_{1-x}$ and Pt layers (see Figure 1), have a strong perpendicular anisotropy. By varying the sputter pressure, the individual layer thicknesses and the thickness of the seedlayer, the magnetic properties of the films can be tailored in such a way that the remanent state after saturation is either single domain (Figure 2) or a fine network of stripe domains (Figure 3). Although films of the second type are clearly not very suitable for magneto-optic recording, they are very interesting for high resolution MFM. For the sample of Figure 3, domains as small as 30 nm have been observed at the MESA laboratory (1 (the number refers to Table 3)) [2]. Therefore this type of layer was taken as a basis for a series of reference sample with varying thickness, as listed in Table 1.

The first reference sample, CAMST reference I, of only 10 bilayers, was chosen to be slightly more demanding to image than the sample of Figure 3. It turned out that this sample was indeed very difficult to measure, and during the first trials only the Basel group (3) succeeded. This is mostly due to the fact that the signals which can be obtained are very low, lower than can be expected from the layer thickness and magnetisation only. The reason for this was not clear and therefore we returned to the original sample of Figure 3 (CAMST reference II) and a sample which was twice as thick (CAMST reference III).

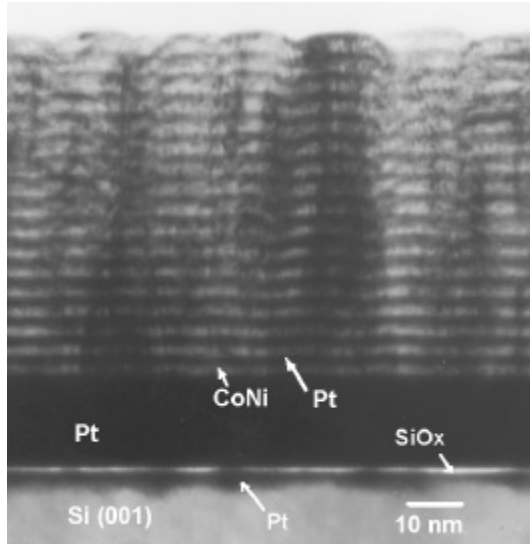


Figure 1 Cross-section TEM image of the layer structure similar to the multilayers used in the CAMST reference samples. The layers are deposited on a Si substrate. The native silicon-oxide layer can clearly be seen. This film consist of 17 bilayers of 3.8 nm $\text{Co}_{50}\text{Ni}_{50}$ and 1.5 nm Pt on top of a 24 nm Pt seedlayer. All layers were deposited at $1.6 \cdot 10^{-2}$ mbar.

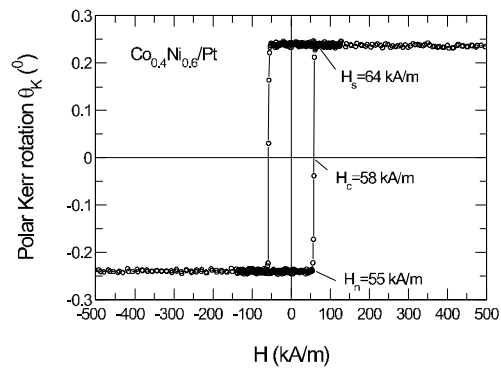
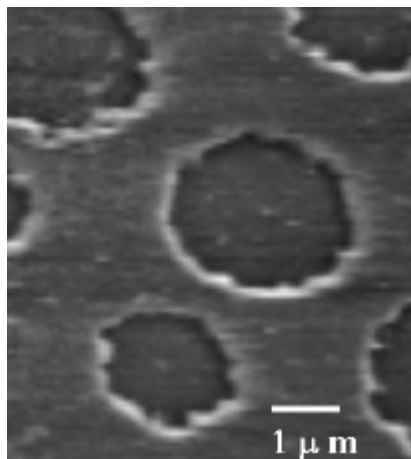


Figure 2 MFM image and MO-Kerr hysteresis loop of a sample with very high squarness which might be suitable for magneto-optic recording, but which is less interesting for MFM. (Composition 10 nm Pt/(0.5 nm $\text{Co}_{40}\text{Ni}_{60}$ /0.5 nm Pt)x10 deposited at $1.6 \cdot 10^{-2}$ mbar). MFM measurement by MESA group (1a)

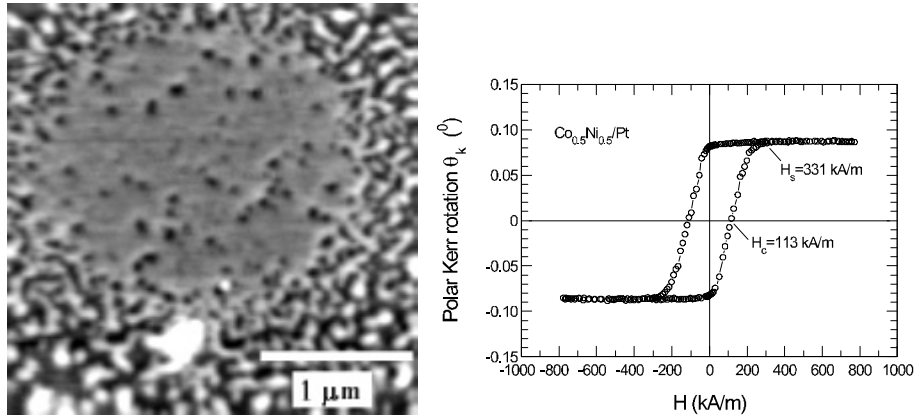


Figure 3 MFM image and MO-Kerr hysteresis loop of a sample with a squareness close, but not equal to one, which is much more interesting for MFM (composition identical to CAMST Reference II). MFM measurement by MESA group (1a)

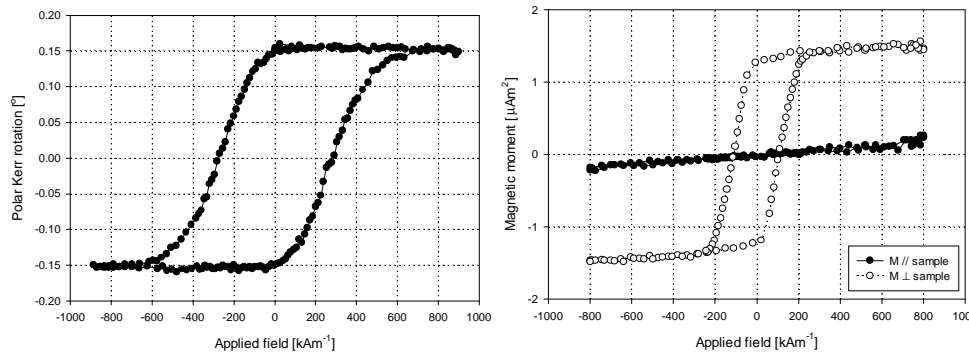


Figure 4 MO-Kerr loop of CAMST reference I and VSM loop of CAMST reference II. The VSM loop shows both the component of the magnetisation parallel to the field (perpendicular to the sample surface) and the component perpendicular to the field (in the sample plane).

Table 1 CAMST Reference Sample structure

CAMST	Number of bilayers	Total layer thickness t [nm]	Material	Co-Ni Thickness [nm]	Pt Thickness [nm]	Seedlayer Thickness [nm]	M_s [MAm ⁻¹]	H_c [kAm ⁻¹]
I	10	13	Co ₄₀ Ni ₆₀	0.5	0.8	9.3	0.33	280 ± 10
II	20	35	Co ₅₀ Ni ₅₀	0.55	1.2	1.2	0.30	90 ± 10
III	40	70	Co ₅₀ Ni ₅₀	0.55	1.2	1.2	0.30	-

4. Thermo-magnetic write experiments

In Figure 4 the perpendicular VSM [3] and MO-Kerr [4] hysteresis loops of CAMST reference II and III are shown. As can be seen the coercivity of these films is fairly high at room temperature. The Curie temperature of these films is however rather low (around 200 °C) because of the addition of Ni, which makes them very easy to use for thermomagnetic writing experiments. The setup used for writing is shown in Figure 5. The 1x1 cm samples are mounted on a rotating disk. A series of bits is written at a particular laser power during one revolution of the disk. Then the lens system is translated over a few microns, and a new track with a different laser power is written. The laser powers were varied such that at the lowest power bits are barely written, whereas at the highest power the bits are clearly visible (see for instance Figure 6c). The laser power sequences are listed in Table 2. Because there is no auto-focusing option to correct for misalignment between the sample surface and the lens trajectory (autofocus), the focus of the laserspot is exact only over a two or three mm region of the sample. Outside this region the smallest bits are not written. This does not impose a problem however because the correct region can easily be identified and selected in the MFM.

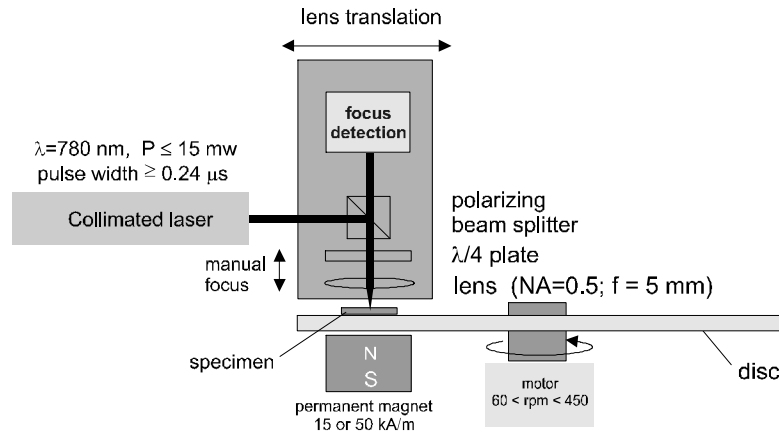


Figure 5 The thermo-magnetic write setup uses a fixed magnetic field of the order of 50 kA/m, the samples are mounted on a rotating disc. The lens translation system is used to write each track at a different laser power [1].

Table 2 Laser powers sequences

Sample	Laser power [mW]
CAMST I	3,5,7,11,3,5,7,11,...
CAMST II	8,10,12,14,12,10,8,...
CAMST III	8,10,12,14,16,14,12,10,8,...

Figure 6 shows overview images of CAMST reference II and III. One can clearly observe the written bit patterns and the fine intrinsic domain structure in the samples. Judging from the distribution of black and white areas in the images, one gets the impression that the overall remanent magnetisation in the regions outside the bits is close to zero; it appears as if the samples have been demagnetized. Prior to writing, the samples are however saturated in a 1.8 T external field perpendicular to the sample plane, and the remanence might naively be expected to be close to 1 as can be seen in the MO-Kerr loops of Figure 3 and Figure 4. Demagnetisation of the samples is probably caused by the rotation above the permanent magnet of the write setup. Since the magnet does not cover the complete disc, only the area under the beam, the sample experiences an alternating field closely resembling a 50 kAm⁻¹ AC demagnetising field.

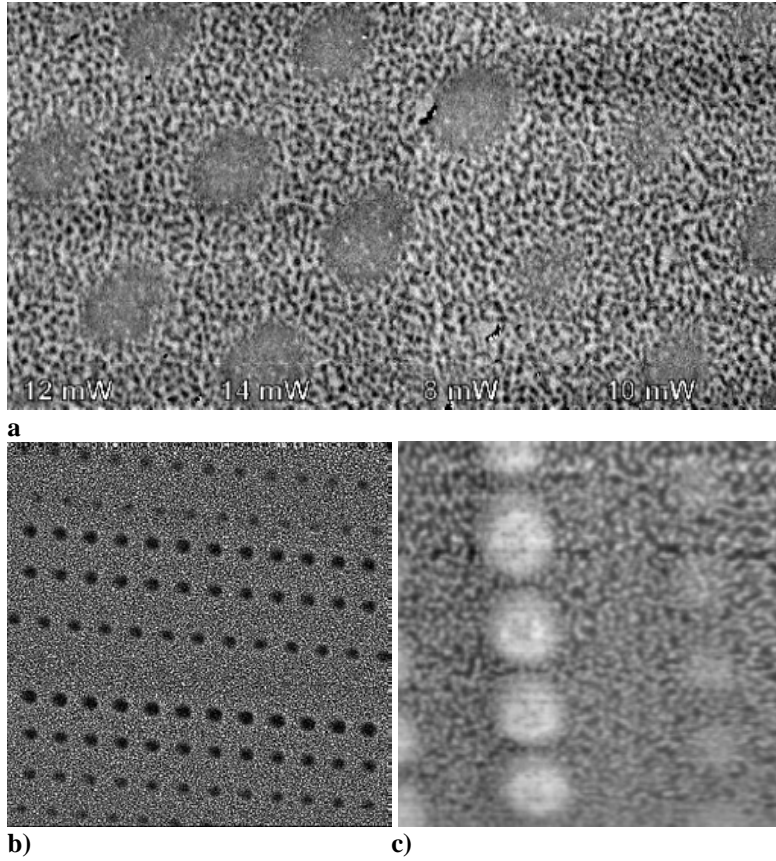


Figure 6 Overview of written tracks on CAMST reference II (a) 20x10 μm by IBM (2) (b) 50x50 nm by NIST (5) and c) CAMST Reference III (10x10 nm by MESA (1b, plane fit method)).

5. Magnetic Force microscopes

The CAMST reference samples were measured in six different laboratories by both commercial and home built instruments. An overview of microscopes, scanning modes, cantilevers and tips is given in Table 3. The first home built MFM of the MESA group (1a) uses a Michelson interferometer [5,6]. The second MESA home built microscope (1b) uses a fiber-optic interferometer sensor [7] and uses design elements of the Basel microscope. Two microscopes are used by the Basel group, the one used for room temperature measurements is the prototype version (3a,b) of a sophisticated low temperature UHV instrument (3c) [8]. However, also the prototype version allows measurements in vacuum.

The SIS microscope (6), makes use as well of a fiber interferometer. The microscope used by the Manchester group (4) uses a heterodyne interferometer [9] and the Digital Instruments systems (2,5,7) use optical beam deflection detection.

Most instruments work at constant tip-to-sample distance (for an overview of methods to keep at constant distance see [2]). The methods used are the relatively simple plane fit procedure (1b,3c), the less straightforward Schönenberger mode of operation (1b, 3a,b) in which the amplitude of cantilever movement due to an oscillating tip-sample voltage is kept constant [10] and the LiftMode operation of the DI instruments which uses a tapping mode AFM measurement to determine the position of the sample surface (2,5,7). Other instruments work at a constant force derivative by keeping the resonance frequency of the cantilever constant (1a, 4). In this case an electrostatic bias force is necessary, which is created by applying a tip/sample voltage.

The microscopes operating in static mode use the soft Si_3N_4 cantilevers (1b, 3), whereas dynamic mode measurement in air are performed with the harder Si cantilevers because they have a higher quality factor (2,4,5,6,7). The dynamic mode measurements presented by the Basel group (3) were performed in vacuum using Si_3N_4 and Si cantilevers. The dynamic mode measurements of Figure 2 and Figure 3 are performed with home made tungsten wire cantilevers with EBID tips (1a).

Both commercially available MFM cantilevers were used as well as commercial cantilevers with home-made coatings or tips (Such as the EBID tip [11])

Table 3 Participating labs

	Institute	Microscope	Measurement mode	Tip
1a	MESA Research Institute, Enschede, NL	Home built, Michelson interferometer	Dynamic mode with phase detection at constant force derivative using electrostatic biasing	20 nm C
1b		Home built, fiber interferometer	Static mode at constant distance using plane fit and Schöenberger method	20 nm C
2	IBM Almaden Research Center, San Jose, USA	Digital Instruments DI5000	Dynamic mode with phase detection at constant distance using LiftMode	30 nm C
2b				Propriet
3a	Institute of Physics, University of Basel, Basel, CH	Home built, fiber interferometer, prototype of 3c, measurements in air	Static mode at constant distance using plane fit and Schöenberger	20 nm C
3b		Home built, fiber interferometer, prototype of 3c, measurements in vacuum	Dynamic mode with frequency detection at constant distance using plane fit and Schöenberger	20 nm C
3c		Home built, fiber interferometer, UHV-LT SFM, measurements in UHV at 7.6K	Dynamic mode with frequency detection at constant distance using plane fit	10 nm F
4	School of Physics, Manchester Metropolitan University, Manchester, UK	Home built, heterodyne interferometer	Dynamic mode with phase detection, constant force derivative using electrostatic biasing	30 nm C
5	NIST, Boulder, USA	Digital Instruments DI3000	Dynamic mode with phase detection at constant distance using LiftMode	30 nm C
6a	Department of Applied Physics, University of Regensburg, Regensburg, D	Surface Imaging Systems	Dynamic mode with amplitude detection keeping damping constant	30 nm
6b				35 nm C
7	Digital Instruments, Santa Barbara, USA	Digital Instruments DI 3100	Dynamic mode with phase detection at constant distance using LiftMode	50 nm C

6. Theoretical modelling of resolution

The CAMST reference samples are useful for testing the resolution of the instruments because they are very flat and consist of stable domains with different sizes. Resolution will therefore be the focus of this paper. There are several ways to define resolution. From a model point of view the minimum detectable wavelength λ_c introduced in [2] is quite useful. This definition is based on a Fourier based description of the imaging in MFM e.g. [12]. This description gives the response of the MFM (force or force derivative) as a function of spatial frequency components in the stray field. Such a response curve, called the tip transfer function (TTF), is given in Figure 8 for a dipole tip model as in shown Figure 7 and for the CAMST reference samples I, II and III. The TTF is repeated here for convenience:

$$F_{mag}(k, z_0) = -\mu_0 \frac{M_s M_t s}{k} e^{-kz_0} (1 - e^{-kt}) \sin(k \frac{b}{2}) (1 - e^{-k\Delta h}) \quad [\text{N}]$$

$$\frac{\mathcal{F} F_{mag}(k, z_0)}{\mathcal{F} k} = -k F_{mag}(k, z_0) \quad [\text{N / m}] \quad (1)$$

The parameters used in the calculation are listed in Table 4. Also shown in Figure 8 are the noise levels caused by the thermal vibration of the cantilevers (so the noise caused by the electronics is neglected). For the static mode and dynamic mode (phase detection) these noise levels are respectively [13],

$$F_{\min} = \sqrt{\frac{4Bck_b T}{w_0 Q}} \quad [\text{N}] \quad (2a)$$

$$\frac{\mathcal{F} F}{\mathcal{F} k}_{\min} = \frac{1}{A_{osc}} \sqrt{\frac{4Bck_b T}{w_0 Q}} \quad [\text{N/m}] \quad (2b).$$

(The noise level for static mode is calculated from $c\sqrt{BN_{th}(0)}$, with N_{th} as in [13]).

The minimum detectable wavelength λ_c is defined by the wavelength at which the signal drops below the noise level at high frequencies. This λ_c is a function of many parameters, the most important being the tip to sample distance z_0 and the tip coating thickness b . Figure 9 shows λ_c as a function of these parameters, all other parameters are as in Table 4. These parameters were chosen to simulate the situation of CAMST Reference II and an EBID tip. For tip-sample distances z_0 larger than the tip coating thickness b , λ_c is almost equal to z_0 . For very small distances λ_c approaches the tip coating thickness b . The difference between static and dynamic mode in air for this set of parameters is negligible. Of course in dynamic mode the electronic noise levels are usually lower, but there is apparently no fundamental advantage of the dynamic mode over the static mode.

Table 4 Parameters used in the calculation of the Tip Transfer Functions and noise levels of Figure 8

M_t	Tip magnetisation	1422 kA/m
b	Tip thickness (coating thickness)	20 nm
s	Tip width	100 nm
Δh	Tip length	1 μ m
M_s	Sample saturation magnetisation	295 kA/m
t	Sample thickness	Table 1
z_0	Tip sample distance	20 nm
c	Cantilever spring constant	0.01 (3 [*]) N/m
f_0	Cantilever resonance frequency	7 (75) kHz
Q	Cantilever quality factor	10 (300)
B	Measurement bandwidth	300 Hz
A_{0sc}	Oscillation amplitude dynamic mode	10 nm

* Values inbetween brackets are for the dynamic mode curves

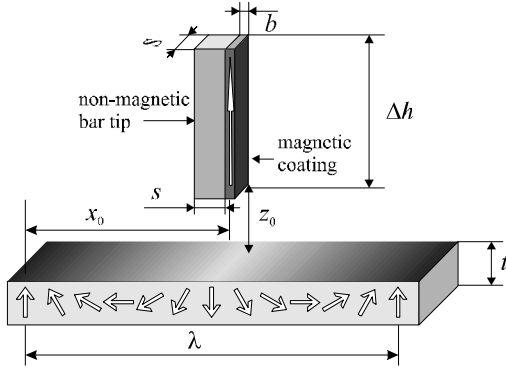


Figure 7 Tip model used in the calculations.

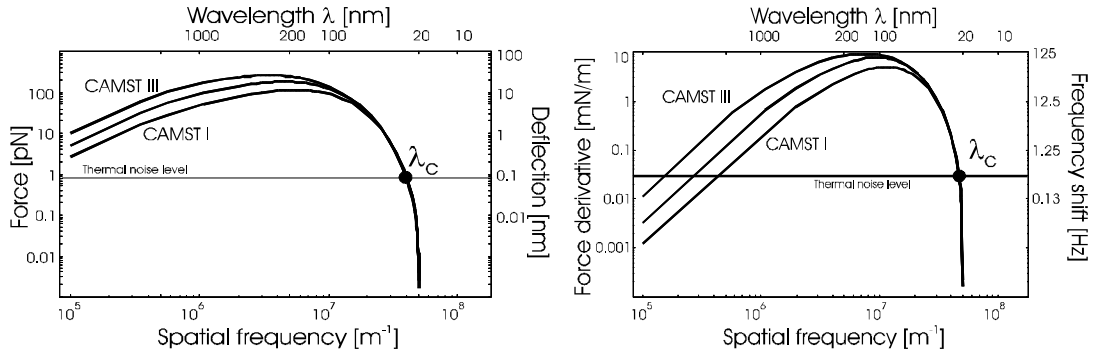


Figure 8 Calculated transfer curves for CAMST reference I, II and III, left static mode, right dynamic mode. Parameters as in Table 4.

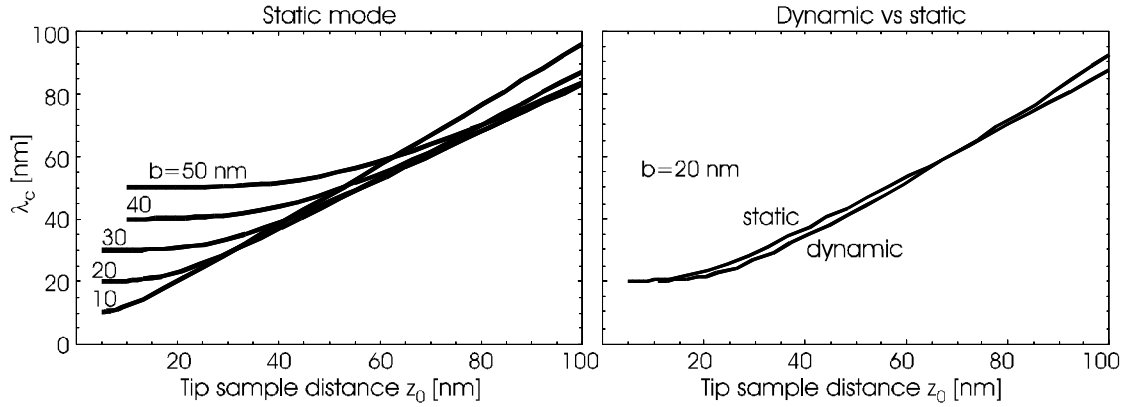


Figure 9 Critical wavelength versus tip-sample distance for different tip coatings. Left static mode, right comparison static and dynamic mode. All other parameters as in Table 4.

7. Measurement results

Figure 10 shows a comparison of MFM images on the same scale of CAMST reference sample I. This sample has a very faint signal and is therefore very difficult to image. Moreover it was only prepared in a very limited quantity and not all laboratories received it. Only the images made by the Digital Instruments systems (2b, 7) approach

the quality of the images of CAMST reference sample II. It appears as if the noise in the system is the factor limiting resolution in this case. Since all participating laboratories measured CAMST Reference sample II, we will focus on that sample here.

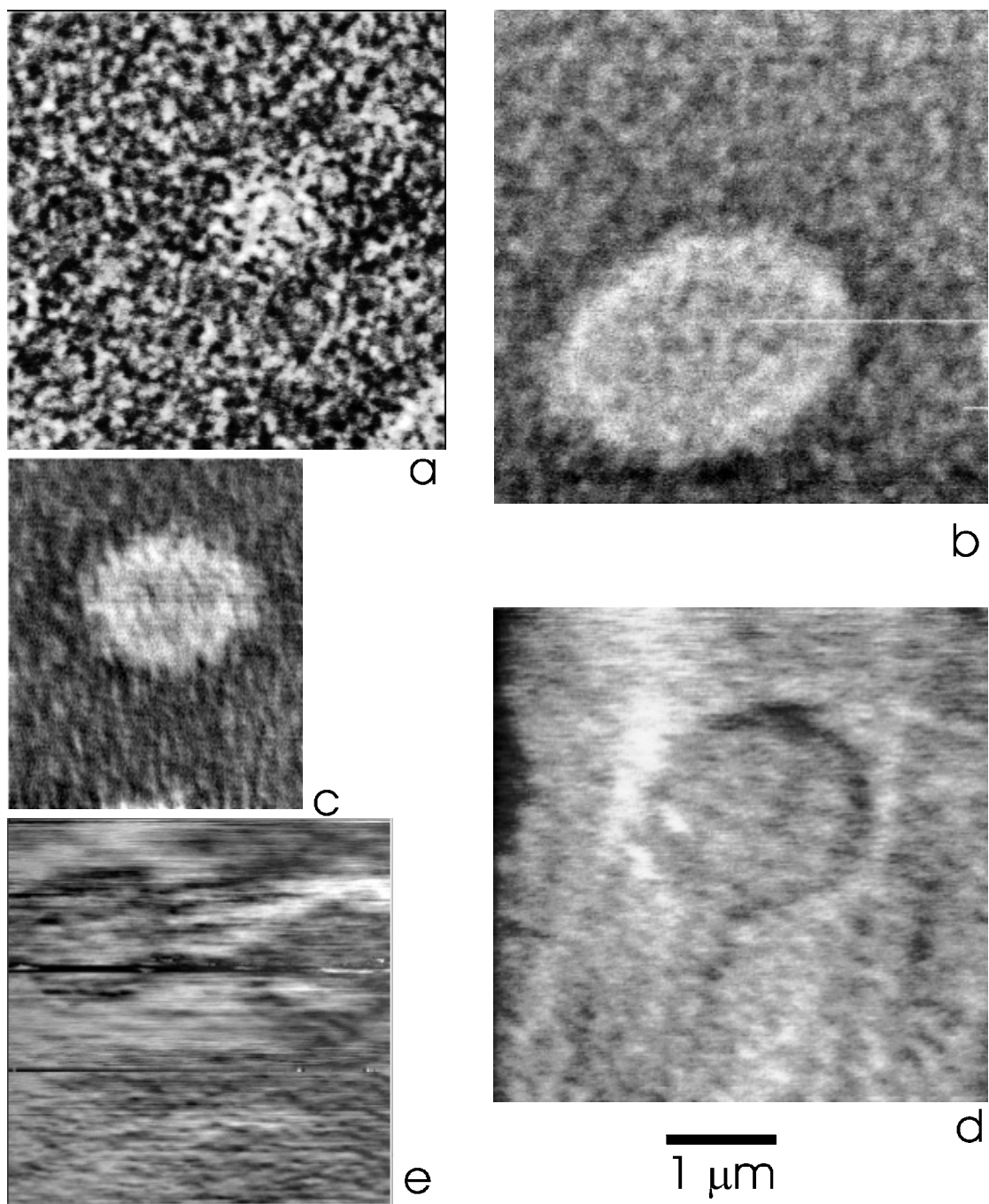


Figure 10 Measurements on CAMST reference I. This sample has only a very faint signal, which results in very noisy images.

- a) Digital Instruments (7)**
- b) IBM DI tip (2b)**
- c) Basel static (3a)**
- d) Regensburg NanoSensors tip (6b)**
- e) MESA planeFit (1b).**

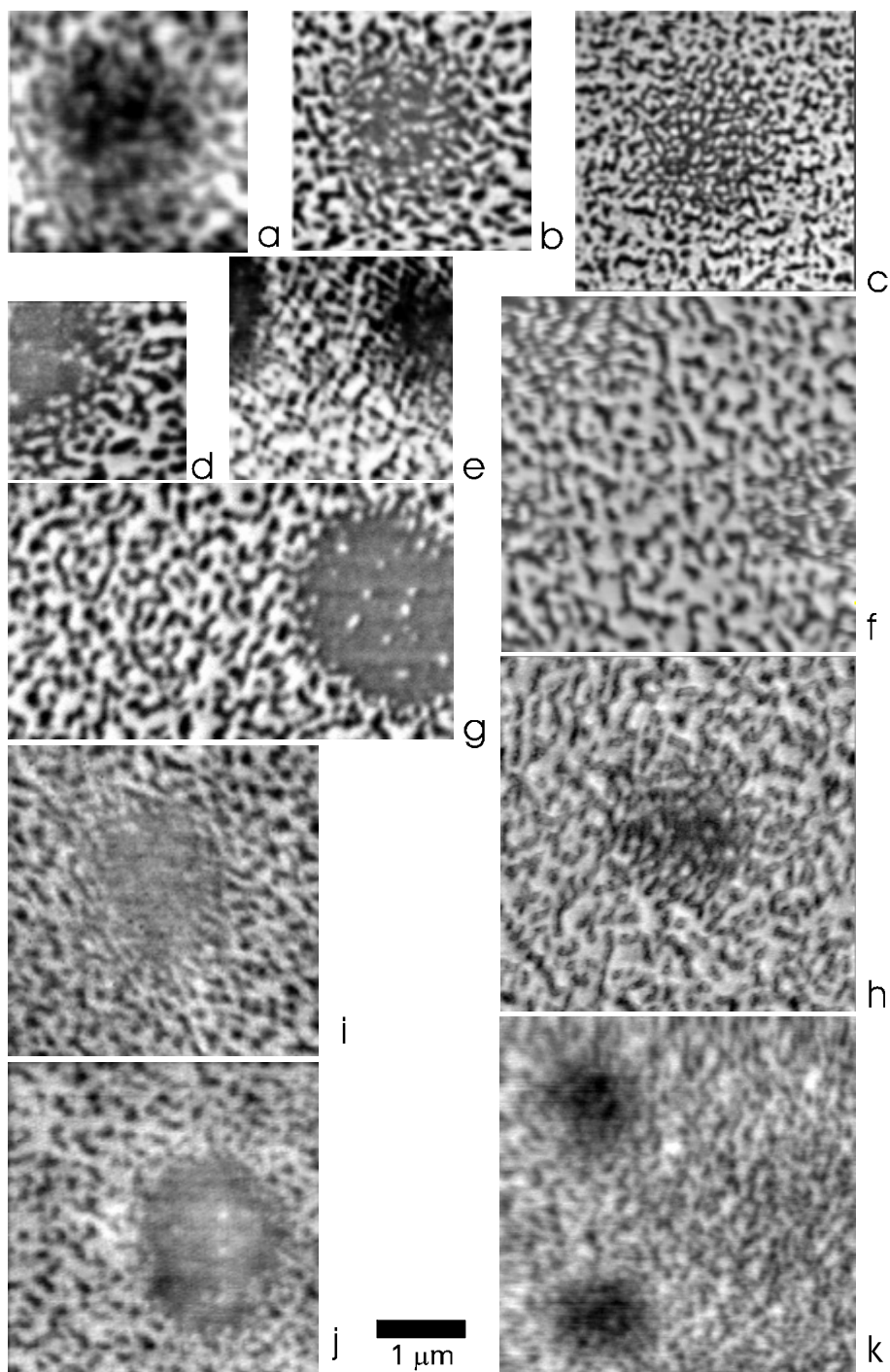


Figure 11 Comparison measurements CAMST II on identical scale

- a) Basel static (3a)**
- b) Basel dynamic (3b)**
- c) Basel dynamic low temperature (3c)**
- d) NIST (5)**
- e) Manchester (4)**
- f) IBM proprietary tip (2a)**
- g) IBM DI tip (2b)**
- h) Digital Instruments (7)**
- i) Regensburg NanoSensors tip (6b)**
- j) Regensburg EBID tip (6a)**
- k) MESA Schönenberger(1b).**

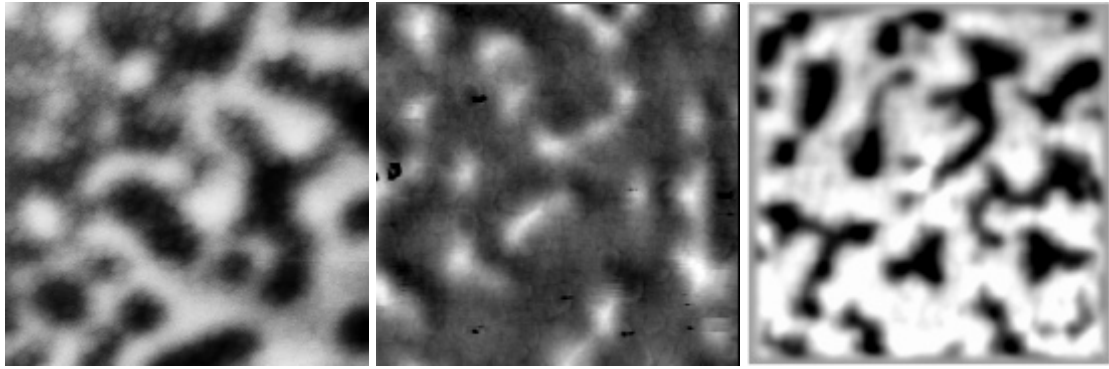


Figure 12 High magnification 1x1 nm scans a) NIST (5) b)IBM proprietary tip (2a) c) Basel, 7.6 K measurement.

Figure 11 shows measurements on the same scale by the different laboratories. The images seem to show almost identical resolution, the distinction lies more in the amount of noise and hum. We tried to two different ways to measure the resolution, namely assessing the smallest detail and the domain transition response.

i) Smallest detail

In this procedure the image is searched for very fine details and then the size of these details is measured by taking the distance between the positions where the signal is half of the maximum signal of the detail (Full Width at Half Maximum, FWHM). It should be noted that not every small detail is truly magnetic. First, if the tip is very close to the surface one can clearly see the topography which has much smaller structures. This might occur especially when using the dynamic operation modes, where one can observe a continuous transition from magnetic to topographic structures as the tip approaches closer to the surface. (Of course also in static mode one will measure topography, for instance because of electrostatic forces, but usually the spatial frequencies are much larger.) Second, the magnetization of the sample might be influenced by the stray field of the tip or vice versa. In some cases one can observe that stray field induced changes in the magnetization of the sample or the tip occur at a reproducible location in the image. Usually such magnetization changes will give rise

to an abrupt change in contrast. Third, depending on the operation mode sharply delineated structures may occur when the tip contacts the surface locally (as seen in Figure 12b). During analysis it was tried to avoid these artefacts by interpreting the image, usually artefacts can clearly be identified.

ii) Domain transition response

In this procedure the image is searched for two adjacent wide domains and the width of the transition is measured by taking the distance between 10% and 90 % of the full step height (Table 5). Note that we do not measure the actual domain wall width, which will of course be much smaller (the width of a Bloch wall in these films would be less than 15 nm). What is measured here is some kind of step response of the TTF.

Table 5 Resolution determined from inspection of the MFM images.

Measurement	Table 3	Figure	FWHM Smallest detail [nm (± 10 nm)]	90/10 % slope [nm (± 10 nm)]
Basel static	3a	Figure 11c	100	90
Basel dynamic	3b	Figure 11b	50	60
Basel dynamic 7.6 K	3c	Figure 11a	30	50
Basel dynamic 1 μ m scan	3c	Figure 12c	30	50
NIST 1 μ m	5	Figure 12a	80	60
NIST 2 μ m	5	Figure 11d	80	60
IBM DI tip	2b	Figure 11g	80	60
IBM Proprietary tip 4 μ m	2a	Figure 11f	70	70
IBM Proprietary tip 1 μ m	2a	Figure 12b	60	50
Manchester	4	Figure 11e	50	40
Regensburg Nanosensors tip	6b	Figure 11i	60	60
Regensburg EBID tip	6a	Figure 11j	90	80
Digital Instruments	7	Figure 11h	70	60
MESA	1	Figure 11k	80	80

8. Conclusions

In conclusion these first results show that the CAMST reference samples are very suitable for testing the maximum resolution obtainable by different MFMs. All images look more or less similar since the appearance of MFM images is determined by the

strongest spatial frequency components, which lie around 100-200 nm for a tip-sample distance of 20 nm. This can be seen in the tip transfer function of Figure 8. (The tip transfer function can be used to flatten the response of the MFM and improve the resolution of the image, as has been shown in [12]). Therefore, the resolution should not be judged from the appearance of the images alone, but a more quantitative method should be used. The results two methods to determine resolution (summarized in Table 5), show that the resolution does not vary considerably between the different instruments, with one exception, for the low temperature measurement by the Basel group. At these low temperatures the noise level is exceptionally low and an excellent signal to noise ratio can be obtained.

One might object that the resolution obtained by the different instruments is almost equal because the sample does not possess any smaller domains. Whilst this might be true in the areas outside the bits, in contrast, at the border of each bit very small domains can be found. Also the “domain wall” measurements indicate that the finest details in the image are not yet revealed. It is expected that in the thinner CAMST reference I the domains might even be smaller, so that this would be the sample to use for exploring the limits of the microscopes.

It seems that as soon as an image can be formed in an MFM, the resolution obtained is well below 100 nm. This is partly caused by the fact that the Tip Transfer Function is very steep on the high frequency side, especially for dynamic mode. Next to this a theoretical analysis indicates that the maximum obtainable resolution appears to be determined by the tip to sample distance. Apparently all microscopes operate at more or less the same tip to sample distance. One should bear in mind that the tip to sample distance of practical importance is the distance between the magnetic charges in the tip and the sample, *not* the physical distance between the two. The distance between the

charges might be larger because not all charges are located at the very end of the tip and due to a non-magnetic surface layer on the sample.

For high resolution it is crucial to reduce the *magnetic* tip to sample distance. The question is whether one should decrease the magnetic tip to sample distance by reducing the physical tip to sample distance or by improving the tip and/or the sample surface. A further point of discussion is how small the physical tip to sample distance can be made. There are several methods to control this physical tip to sample distance, but it is doubtful whether one can get arbitrarily close. At a certain distance the force derivative of the VanderWaals forces will become larger than the cantilever spring constant, and the tip will be pulled into the sample. Also the water film on the surface might play a role. But even so, the physical tip to sample distance can become very small. Calculations predict a distance of the order of a few nm if very hard cantilevers are used (5 N/m) [14]. Using the LiftMode technique, it is for instance possible to almost hit the surface. In this case the tip to sample distance is determined by the cantilever vibration amplitude, which can be much smaller than the resolution obtained in the measurements presented here. If the theory on resolution is correct, this would mean that the separation between the charges in the tip and the sample is about 50 nm. This would imply that an improvement of resolution should be obtained by improving the tip, working with very clean samples and possibly operating in vacuum to remove the water film.

If on the other hand the physical tip to sample distance is not very small, resolution can be improved by getting closer to the sample. In this respect the constant force derivative (CFD) mode has an advantage over the constant distance (CD) mode. In the CFD mode the tip to sample distance can be very small for repelling forces on the tip. This might be the reason why the CFD images of the Manchester group (4) show such

a good resolution when looking at small details. Also the CFD image of Figure 3 has a very high resolution. A drawback of the CFD mode is that the tip sample distance in the attracting regions of the sample is increased, which will decrease resolution. So for the analysis of images the CD mode is to be preferred.

The authors are aware that a similar program on an MFM reference sample, the NIST reference sample, exists [15]. Both reference samples are however compatible, the NIST reference sample being more suitable for calibration of the stray fields whereas the CAMST reference samples are more suitable for testing resolution.

9. Acknowledgements

The authors wish to acknowledge the CAMST program for allowing us to initialize this project, Dr Meng Qi for figures 1 to 3 and dr. P. Rice for MFM measurements. The research of Dr. Abelmann has been made possible by a fellowship of the Royal Netherlands Academy of Arts and Sciences.

10. References

- [1] Q. Meng, D. M. Donnet, P. J. A. Schendel van, J. C. Lodder, and T. J. Popma, A, *J Magn Soc Jpn*, vol. 20, (1996), 53
- [2] S. Porthun, L. Abelmann, and J. C. Lodder, *J. Magn. Magn. Mater.*, vol. 182, (1998), 238
- [3] B. D. Cullity, *Introduction to Magnetic Materials*, New York: Addison-Wesley Publ. Comp. (1972),
- [4] W. P. Vandrent, T. Suzuki, Q. Meng, J. C. Lodder, and Th J. A. Popma, *J Appl Phys*, vol. 76, (1996), 6190
- [5] A. J. den Boef, *Appl. Phys. Let.*, vol. 55, (1989), 439

- [6] A. J. den Boef, Scanning force microscopy using optical interferometry (1991), University of Twente.
- [7] A. Moser, H. J. Hug, Th Jung, U. D. Schwarz, and H.-J. Guentherodt, *Meas Sci Technol*, vol. 4, (1993), 769
- [8] H. J. Hug, B. Stiefel, P. J. A. Schendel van, O. Knauf, A. Moser, S. Martin, and H.-J. Guentherodt, *In preparation*, vol. (1998),
- [9] M. S. Valera and A. N. Farley, *Meas Sci Technol*, vol. 7, (1996), 30
- [10] C. Schonenberger, S. F. Alvarado, S. E. Lambert, and I. L. Saunders, *J Appl Phys*, vol. 67, (1990), 7278
- [11] M. Ruhrig, S. Porthun, J. C. Lodder, S. McVitie, L. J. Heyderman, A. B. Johnston, and J. N. Chapman, *J Appl Phys*, vol. 79, (1996), 2913
- [12] H. J. Hug, B. Stiefel, P. J. A. Schendel van, A. Moser, R. Hofer, H.-J. Guentherodt, S. Porthun, L. Abelmann, J. C. Lodder, G. Bochi, and R. C. O'Handley, *accepted for publication in J Appl Phys* vol. (1998),
- [13] T. R. Albrecht, P. Grutter, D. Horne, and D. Rugar, *J Appl Phys*, vol. 69, (1991), 668
- [14] S. Porthun, L. Abelmann, S. J. L. Vellekoop, J. C. Lodder, and H. J. Hug, *J Appl Phys*, vol. 66, (1998), S1185
- [15] P. Rice, S. E. Russek, and B. Haines, *IEEE Trans Magn*, vol. 32, (1996), 4133